Time-Resolved Fluorescence Anisotropy of Fluorescent-Labeled Lysophospholipid and Taurodeoxycholate Aggregates

Laura J. DeLong and J. Wylie Nichols
Department of Physiology, Emory University School of Medicine, Atlanta, Georgia 30322 USA

ABSTRACT Previous work from this laboratory demonstrated that the environment-sensitive lysolipid *N*-(7-nitrobenz-2-oxa-1,3-diazol-4-yl)-monomyristoylphosphatidylethanolamine (*N*-NBD-MPE), at concentrations below its critical micelle concentration ($CMC_{N\text{-}NBD\text{-}MPE}$ = 4 μM), reached maximum fluorescence yield upon the addition of taurodeoxycholate (TDC) at concentrations well below its CMC (CMC_{TDC} = 2.5 mM). These data indicated the formation of micellar aggregates of the two amphiphiles at concentrations below both of their CMCs. In the present study, fluorescence lifetime and differential polarization measurements were made to determine the size of these aggregates. In the absence of TDC and at 0.5 mM TDC a single lifetime (τ) and rotational correlation time (ϕ) were measured for *N*-NBD-MPE at the submicellar concentration of 2 μM, indicating a lack of interaction between the two molecules at this concentration. Above 0.5 mM TDC, two discrete lifetimes were resolved. Based on these lifetimes, two distinct rotational correlation times were established through polarization measurements. The shorter ϕ (0.19–0.73 ns) was ascribed to local probe motions, whereas the longer ϕ was in a time range expected for global rotation of aggregates the size of simple bile salt micelles (3–6.5 ns). From the longer ϕ, molecular volume and hydrodynamic radii were calculated, ranging from ~15 Å at 1 mM to ~18 Å at 5 mM TDC. These data support the conclusion that monomeric lysolipids in solution seed the aggregation of numerous TDC molecules (aggregation number = 16 at 1 mM TDC) to form a TDC micelle with a lysolipid core at concentrations below which they both self-aggregate.

INTRODUCTION

Bile salts facilitate the absorption of amphiphilic lipids (e.g., cholesterol, phospholipids, fatty acids, lysophospholipids, and fat soluble vitamins) from the intestine by their ability to form mixed micelles, which facilitate amphiphile transfer to the surface of mucosal cells lining the small intestine (Carey et al., 1983; Erlinger, 1987; Wilson, 1971, 1991). Absorption of these slightly water-soluble amphiphiles is thought to occur by transfer from the mixed micelles through the water to the enterocyte cell surface (Westergaard and Dietschy, 1976). One of the primary ways in which bile salt mixed micelles facilitate lipid absorption is by providing a pathway of diffusion that acts in parallel to the diffusion of free monomers through the unstirred water layer. In this way, bile salt mixed micelles effectively reduce the diffusional boundary layer resistance and increase the rate of absorption.

Work from this laboratory (Nichols, 1986, 1988) has demonstrated another important property of bile salts that is relevant to their ability to facilitate lipid absorption. Kinetic measurements of the transfer of fluorescent-labeled phospholipids between bile salt/phospholipid mixed micelles or vesicles demonstrated that the rate of phospholipid transfer through the water phase is significantly faster than transfer between phospholipid vesicles in the absence of bile salts. Subsequent work has led to the hypothesis that the faster rate of phospholipid transfer in the presence of bile salts is due to the ability of water-soluble, monomeric phospholipids to seed the formation of bile salt micelles. These seeded micelles coexist in equilibrium with mixed micelles and vesicles in bile salt/phospholipid mixtures and function as shuttle carriers to increase the rate of exchange (Shoemaker and Nichols, 1990, 1992). This hypothesis is based on the demonstration that bile salts and lysophospholipids form micelles at concentrations below both of their critical micelle concentrations (Shoemaker and Nichols, 1990) and that these micelles increase the rate of lysophospholipid removal from and insertion into vesicle bilayers (Shoemaker and Nichols, 1992).

To gain further information regarding the molecular nature of micelle formation between bile salts and lysophospholipids at concentrations below both of their CMCs, we have used time-resolved fluorescence to measure the lifetimes and rotational correlation times of the environment-sensitive, fluorescently labeled lysophospholipid, *N*-(7-nitrobenz-2-oxa-1,3-diazol-4-yl)-monomyristoylphosphatidylethanolamine (*N*-NBD-MPE) in association with the bile salt taurodeoxycholate. Hydrodynamic radii for simple bile salt micelles have been determined previously by using light scattering techniques (Mazer, 1990; Schurtenberger et al., 1985) and for bile salt-phospholipid mixed micelles by using high-performance liquid chromatography (Nichols and Ozarowski, 1990), small-angle neutron scattering (Long et al., 1994; Hjelm et al., 1988, 1990), small-angle x-ray scattering (Müller, 1981, 1984), and nuclear magnetic resonance (Schurtenberger and Lindman, 1985). The measurement of fluorescence lifetimes and rotational correlation times of mixed *N*-NBD-MPE/TDC micelles allowed the investigation of environmental and motional

Received for publication 11 August 1995 and in final form 12 December 1995.

Address reprint requests to Dr. J. Wylie Nichols, Department of Physiology, Emory University School of Medicine, Atlanta, GA 30322. Tel.: 404-727-7422; Fax: 404-727-2648; E-mail: wnichols@physio.emory.edu.

0006-3495/96/03/1466/06 $2.00

properties that exist at very low bile salt concentrations or coexist with simple TDC micelles at higher concentrations. These measurements confirmed the aggregation of *N*-NBD-MPE and TDC at concentrations below both of their CMCs and provided an estimate of the minimum stoichiometry of ~16 TDC molecules per molecule of *N*-NBD-MPE.

MATERIALS AND METHODS

Solutions and preparations

The sodium salt of taurodeoxycholate (Sigma Chemical Co., St. Louis, MO) was analyzed for >95% purity via thin-layer chromatography. *N*-NBD-MPE was prepared by the reaction of monomyristoylphosphatidylethanolamine with NBD chloride (4-chloro-7-nitrobenz-2-oxa-1,3-diazole) (Avanti Polar Lipids, Alabaster, AL) (Struck et al., 1981), purified by preparative thin-layer chromatography on silica plates and stored at −20°C in $CHCl_3$. Solutions of TDC were prepared in HEPES-buffered saline (HBS) (150 mM NaCl (Fisher Biotech, Fair Lawn, NJ), 0.04% NaN_3 (Sigma Chemical Co.), 10 mM HEPES (Fisher Biotech), pH 7.4). Mixtures of TDC and *N*-NBD-MPE were prepared by the addition of the appropriate concentration of TDC in HBS to a test tube containing dried and desiccated *N*-NBD-MPE. $CHCl_3$ was removed by evaporation with a steady stream of N_2 followed by 4–12 h of vacuum desiccation. Phospholipid concentrations were determined with a lipid phosphorous assay (Ames and Dubin, 1960).

Fluorescence measurements

NBD fluorescence lifetimes and differential polarization measurements were collected by using a multifrequency phase and modulation fluorometer based on the design of Gratton (Gratton and Limkeman, 1983). Briefly, the excitation intensity is modulated sinusoidally through a frequency in the megahertz range, resulting in a modulated fluorescence emission delayed in phase because of the lifetime of the excited state. Sample lifetimes are then determined by the relative phase shift and demodulation of the fluorescence with respect to a fluorescent standard. The relationships between the phase shift and the modulation ratio and their lifetimes are as follows:

$$\tan P = \omega\tau_p$$

$$M = [1 + (\omega\tau_m)^2]^{-1/2},$$

where P is the phase shift, M the relative modulation, ω the angular modulation frequency, and τ_p and τ_m the phase and modulation lifetimes, respectively. Depending upon the frequency, these two lifetimes will yield different values in a multicomponent system, affecting the weighting of components, lifetimes, and fractional intensities (Hazlett et al., 1993).

The excitation light for the NBD-lysolipids was provided by a tunable mode-locked ND:YAG (Coherent Antares Model 76, Palo Alto, CA) pumped, cavity dumped DCM dye laser (Coherent model 700). The 690-nm beam was frequency doubled to obtain the 345-nm wavelength beam. The excitation light passed through a U360 broad bandpass filter, and the fluorescence emission was monitored through a KV450 cutoff filter. The frequency range for the lifetime measurements was 7.620–251.46 MHz, and the range for the polarization measurements was 3.81–300.99 MHz. The fluorescent standard used was POPOP (Eastman-Kodak, Rochester, NY).

Data collection and initial analysis were performed with ISS software (ISS, Champaign, IL). χ^2 values indicate the goodness of fit for the decay models defined as

$$x^2 = \sum\{[(P_c - P_e)/\sigma_p] + [(M_c - M_e)/\sigma_m]\}^2/(2n - f - 1),$$

where P and M correspond to the phase shift and relative modulation values and c and e subscripts indicate calculated and experimental values. n is the number of modulation frequencies, and f is the number of free parameters. σ_p and σ_m indicate the phase and modulation standard deviations, respectively, which were set constant at values of 0.004 for the modulation and 0.2° for the phase shift (Jameson et al., 1984).

Steady-state polarization measurements were performed in the T format on an SLM 8000C spectrofluorometer (SLM Instruments, Urbana, IL). NBD fluorescence was excited at 475 nm (8-nm slit width). The vertical and horizontal components of the emitted fluorescence were measured simultaneously by two photomultiplier tubes mounted at right angles to the excitation light beam. Emitted light was filtered through a 500-nm longpass cutoff filter and either a vertically or horizontally oriented Glan-Thompson polarizer. To measure polarization (P), the intensity (I) of the vertical (v) and horizontal (h) components of the emitted fluorescence were measured with the excitation polarizer in the vertical position and ratioed (I_v/I_{hv}). A correction factor for the instrument was obtained by measuring the ratio of the vertical and horizontal emitted components with the excitation polarizer set in the horizontal position (I_{vh}/I_{hh}). Polarization is calculated using the following equation:

$$P = \frac{(I_{vv}/I_{hv})/(I_{vh}/I_{hh}) - 1}{(I_{vv}/I_{hv})/(I_{vh}/I_{hh}) + 1}.$$

Background signals for the instrument and the TDC/HEPES buffer solutions were automatically subtracted for each polarization measurement. At least 10 measurements were made per sample.

The steady-state limiting polarization for the free, dilute *N*-NBD-MPE in vitrified solution (P_0) was determined to be 0.31 in 70% glycerol at −4°C. Under these conditions, the fluorophore does not rotate appreciably during the lifetime of the excited state. Thus, P_0 is a measure of the intrinsic polarization of the *N*-NBD-MPE molecule, resulting from angular displacement between the excitation and emission transition moments, and represents the maximum expected value of polarization.

RESULTS AND DISCUSSION

The fluorescence intensity of monomeric, water-soluble *N*-NBD-MPE has previously been shown to increase as a function of TDC concentration and to reach a maximum at concentrations below the CMC of TDC (Shoemaker and Nichols, 1990; reproduced in Fig. 1 E). These data indicated that the association of TDC molecules with *N*-NBD-MPE increased the hydrophobicity of the environment surrounding the probe and that the maximum hydrophobic environment was achieved at TDC concentrations below its CMC. To determine the size and molecular stoichiometry of these micelles that form when both *N*-NBD-MPE and TDC are below their respective CMCs, we used multifrequency phase and modulation fluorometry to measure the lifetimes and rotational correlation times of the *N*-NBD-MPE molecule in the presence of TDC. The *N*-NBD-MPE concentration was held constant at 2 μM, well below its CMC of 4 μM (Shoemaker and Nichols, 1990). TDC concentrations were varied from below to above its CMC of 2.5 mM (Shoemaker and Nichols, 1990).

Measurements of the relative phase shift and demodulation of *N*-NBD-MPE fluorescence in these mixtures were found to fit best to a single lifetime at 0.5 mM TDC and to fit best to two lifetimes at all higher concentrations (Table 1). Fitting to a Lorentzian distribution was also attempted but did not improve the χ^2 fit parameter. The presence of a single lifetime at 0.5

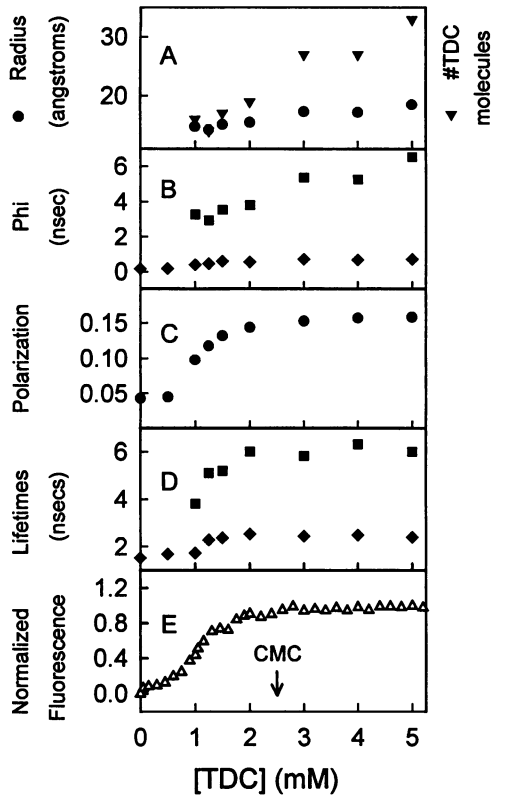

FIGURE 1 (*A*) Radius (●) and no. of TDC molecules (▼) per aggregate versus TDC concentration. See text for details on calculations. (*B*) Variation of rotational correlation times, ϕ_1 and ϕ_2 with TDC concentration. The ϕ values plotted are from Table 2. ϕ_1, ◆; ϕ_2, ■. (*C*) Steady-state polarization versus [TDC]. The standard deviation for each point is ±0.002. (*D*) Dependence of the lifetimes on the concentration of TDC. The values plotted are those from Table 1. τ_1, ◆; τ_2, ■. (*E*) Dependence of the steady-state fluorescence of *N*-NBD-MPE on TDC concentration (reproduced from Shoemaker and Nichols, 1990). The critical micelle concentration shown was determined by light scattering. All data (*A–D*) were taken at T = 20°C, pH = 7.4. The frequency range was 7.620–251.6 MHz for the lifetime data and 3.81–300.99 MHz for the differential phase data.

mM TDC was consistent with the fluorophore residing in a single environment arising from a free probe in solution. The two discrete lifetimes obtained at 1 mM TDC and above indicated that the NBD fluorophore was experiencing two different environments. Both lifetimes increased with increasing TDC concentration, indicating a transition of the probe from soluble monomer to association with TDC in micelles. Consistent with the steady-state fluorescence measurements, this transition occurred at concentrations below the CMC of TDC. At 1 mM TDC, two lifetimes were observed; however, the shorter of the two was essentially the same as that measured for free monomer at 0.5 mM. These data argue that approximately half of the *N*-NBD-MPE was water soluble and half was TDC micelle associated at this concentration. Above 1 mM both lifetimes increased to constant levels, reflecting two distinct environments for the NBD fluorophore in the micelles. The nature of these two distinct environments is not known; however, the existence of two lifetimes for NBD-labeled phospholipids has been observed previously in liposomes (Arvinte et al., 1986; Horowitz et al., 1992). Another study suggested that a shorter lifetime results from self-quenching of the NBD moiety attached to phosphatidylserine in phospholipid vesicles (Hoekstra, 1982). Given the low, submicellar concentration of *N*-NBD-MPE and the large excess of TDC used in these experiments, self-quenching is not a likely explanation for the shorter lifetime observed in these experiments.

Differential polarization measurements were made to determine the rotational correlation times (ϕ) for *N*-NBD-MPE in the TDC solutions. The differential phase and modulation data for the TDC aggregates was found to fit best to a single discrete ϕ value at 0.5 mM TDC and to two ϕ values at higher concentrations (Table 2).

The single rotational correlation time measured at 0.5 mM TDC indicated that the fluorophore has a single rotational element. Furthermore, its magnitude (0.2 ns) was consistent with that predicted for the free rotation of *N*-NBD-MPE in solution. The existence of two discrete rotational correlation times at concentrations above 0.5 mM

TABLE 1. Fluorescence lifetimes (τ) for *N*-NBD-MPE in the presence of TDC

[TDC] (mM)	τ_1 (ns)	τ_2 (ns)	f_1	χ^2
0.0	1.53	—	1.00	3.3
0.5*	1.70 ± 0.02	—	1.00	5.1
1.0¶	1.74 ± 0.14	3.82 ± 0.25	0.53 ± 0.07	2.8
1.25‡	2.29 ± 0.16	5.11 ± 0.61	0.66 ± 0.06	3.2
1.5‡	2.37 ± 0.12	5.20 ± 0.36	0.62 ± 0.02	3.2
2.0*	2.53 ± 0.03	6.01 ± 0.16	0.64 ± 0.01	2.8
3.0*	2.45 ± 0.04	5.83 ± 0.16	0.55 ± 0.01	4.6
4.0*	2.50 ± 0.03	6.32 ± 0.17	0.57 ± 0.01	3.6
5.0§	2.41 ± 0.07	6.01 ± 0.13	0.53 ± 0.03	3.0

The lifetimes were determined with the ISS software. [*N*-NBD-MPE] was held constant at 2μM over the TDC concentration range. T = 20°C, Ex=345 nm. f_1 is the fractional intensity for τ_1. χ^2 is the goodness of fit as defined in Materials and Methods. A data set is defined as single set of lifetime and polarization measurements of differential phase and modulation data for a particular sample.

* Representative data set.

‡ Two data sets.

§ Three data sets.

¶ Four data sets.

TABLE 2. Rotational correlation times (ϕ) for *N*-NBD-MPE in the presence of TDC

[TDC] (mM)	ϕ_1 (ns)	ϕ_2 (ns)	f_1	χ^2
0.0	0.18 ± 0.02		1.00	4.5
0.5	0.19 ± 0.01		1.00	3.5
1.0	0.41 ± 0.02	3.3 ± 0.2	0.66 ± 0.01	1.9
1.25	0.46 ± 0.01	2.9 ± 0.1	0.60 ± 0.004	0.7
1.5	0.61 ± 0.02	3.5 ± 0.1	0.62 ± 0.01	0.9
2.0	0.56 ± 0.02	3.8 ± 0.1	0.53 ± 0.02	1.1
3.0	0.73 ± 0.03	5.4 ± 0.3	0.58 ± 0.01	1.5
4.0	0.68 ± 0.02	5.3 ± 0.2	0.55 ± 0.01	1.2
5.0	0.73 ± 0.03	6.5 ± 0.4	0.58 ± 0.01	1.6

Rotational correlation times for the TDC aggregates at 20°C were determined with the ISS software using a set of lifetimes determined from the ISS software. Ex = 345 nm. f_1 is the fractional anisotropy amplitude of ϕ_1. χ^2 is the goodness of fit as defined in Materials and Methods. All numbers were determined from a single set of lifetime data. r_o was not fixed and ranged between 0.235 and 0.292.

implied that there were at least two distinct motions associated with *N*-NBD-MPE in the TDC aggregate. The longer rotational correlation times (ϕ_2) (Table 2) were in the same range as that predicted from the size of simple TDC micelles (16–22 Å; Mazer, 1990) and therefore were assigned to the global rotation of the aggregates. The shorter rotational correlation times (ϕ_1) (Table 2) were longer than that predicted for free probe in solution and were therefore more likely to reflect local probe rotations such as phosphate headgroup wobbling, which has been reported to be on the order of 10^{-9} s (Milburn and Jeffrey, 1987, 1989).

The dependence of both rotational correlation times (ϕ_1 and ϕ_2) on the concentration of TDC is plotted in Fig. 1 *B*. At 1 mM TDC, which was the lowest TDC concentration that resulted in two rotational correlation times, the longer of the two (ϕ_2) was 3.3 ns, reflecting the global rotation of an aggregate with a hydrodynamic radius of 14.7 Å (Table 3; Fig. 1 *A*). The rotational correlation time (ϕ_2) increased gradually as the TDC concentration was increased above 1 mM, suggesting a gradual increase in aggregate size. However, because the steady-state polarization measurements (Fig. 1 *C*) demonstrated a constant aggregate size at concentrations above 2 mM TDC, ϕ_2 most likely approached a constant magnitude at higher TDC concentrations. ϕ_1 also reached a maximum at TDC concentrations above 1.5 mM, reflecting maximum restriction of the local motions of NBD by the association of TDC molecules well below its CMC.

The molar volumes, radii, and stoichiometry of the *N*-NBD-MPE/TDC aggregates predicted from ϕ_2 are presented in Table 3 and plotted in Fig. 1 *A*. The hydrodynamic radii ranged from 14.1 Å below the CMC to 18.4 Å above, which was in the size range predicted for simple TDC micelles by light scattering (16–22 Å; Mazer, 1990).

Using an anhydrous molecular volume of 770 Å^3 for TDC estimated from molecular dimensions (Small, 1971) and 650 Å^3 for *N*-NBD-MPE estimated from the crystal unit cell of monopalmitoylphosphatidylethanolamine (Pascher et al., 1992), and assuming one *N*-NBD-MPE molecule per aggregate, the number of TDC molecules per aggregate was calculated to be between 16–19 below the CMC of TDC and 27–33 above. This number agrees with previous light scattering studies in which an aggregation number of 10–25 was predicted for simple TDC micelles (Mazer, 1990). These estimates do not take into account the packing geometry or the degree of hydration of the molecules in the aggregate, which could affect the calculated aggregation number by one or two molecules.

These experiments indicated that at TDC concentrations well below its CMC, relatively large aggregates of TDC formed around the *N*-NBD-MPE molecules. Steady-state fluorescence measurements (Shoemaker and Nichols, 1990) demonstrated that the NBD chloride did not associate with TDC molecules at concentrations below its CMC. Furthermore, as the acyl chain length of the *N*-NBD-PE molecules increased from 12 carbons to 18 carbons, the TDC concentration at

TABLE 3. Calculated molecular volumes, radii, and TDC stoichiometry of *N*-NBD-MPE/TDC aggregates

[TDC] (mM)	ϕ_2 (ns)	V(cm^3/mol)	r(Å)	No. of TDC molecules
1	3.3	13,300	14.7	16
1.25	2.9	11,700	14.1	14
1.5	3.5	14,100	15.0	17
2	3.8	15,300	15.4	19
3	5.4	21,800	17.3	27
4	5.3	21,400	17.2	27
5	6.5	26,200	18.4	33

Molecular volumes were calculated from ϕ_2 using the equation $V = \phi RT/\eta N_A$, where V is the molecular volume, R is the ideal gas constant, T is the absolute temperature, η is the viscosity of the solvent (assumed to be 0.01018 poise for 0.15 M NaCl solution at 20°C), and N_A is Avogadro's number. Hydrodynamic radii were calculated from V, assuming spherical shaped aggregates. The number of bile salt molecules was determined by assigning one lysolipid molecule per aggregate and using the following equation: No. of TDC molecules = $(V_{aggregate} - V_{N\text{-NBD-MPE}})/V_{TDC}$.

which the *N*-NBD-lysolipids associated with TDC decreased. These data argued that the acyl chain regions of the *N*-NBD-lysolipids induced the aggregation of TDC molecules. This aggregation occurred with high cooperativity, resulting in relatively large micelles (aggregation number 16–19 TDC molecules) at concentrations well below the CMC of TDC.

The lifetime data at 1 mM TDC indicated that approximately 50% of the *N*-NBD-MPE was associated with TDC micelles and half was free in solution. This result argued that the increase in steady-state fluorescence as TDC was added to *N*-NBD-MPE (Fig. 1 *E*) did not occur by gradual addition of TDC to all *N*-NBD-MPE molecules, but rather by inducing, with high cooperativity, the aggregation of TDC to form micelles with a lysolipid core, leaving the remaining *N*-NBD-MPE free in solution.

SIGNIFICANCE

These data demonstrated that the hydrophobic acyl chain region of water-soluble lysolipid molecules acts to seed the aggregation of 16–19 TDC molecules at concentrations below their CMC. Previous studies demonstrated that these seeded micelles coexist with bilayer vesicles and interact with the vesicles to facilitate *N*-NBD-lysoPE removal from and insertion into phospholipid vesicles (Shoemaker and Nichols, 1992). Given that the seeding of bile salt aggregation appears to be a nonspecific hydrophobic interaction, it is likely to be a generalized phenomenon affected by any number of different amphiphiles. Thus, we suggest that the formation of small aggregates of bile salts surrounding a single, water-soluble amphiphile will increase its effective water-soluble concentration and thereby increase its transfer rate through the water phase. This phenomenon provides an additional mechanism by which bile salts facilitate amphiphile absorption in the intestine.

These observations are of general interest as an example of the aggregation behavior of mixed amphiphiles in solution. Although it is known that the CMCs of binary mixtures of amphiphiles are intermediate in value to the respective CMCs of the two amphiphiles, the data presented herein demonstrate that mixed micelles form at concentrations below the CMCs of both amphiphiles. It remains to be determined whether this is a unique property of the bile salts or of amphiphiles in general.

We thank Theodore Hazlett for his assistance and advice with the time-resolved anisotropy measurements.

This work was supported by National Institutes of Health Grant R01-DK 40641-05 to JWN. The experiments and analyses of the fluorescence data were performed at the Laboratory for Fluorescence Dynamics (LFD) at the University of Illinois at Urbana-Champaign (UIUC). The LFD is supported jointly by the Division of Research Resources of the National Institutes of Health (RRO3155-01) and UIUC.

REFERENCES

Ames, B. N., and D. T. Dubin. 1960. The role of in the neutralization of bacteriophage deoxyribonucleic acid. *J. Biol. Chem.* 235:769–775.

Arvinte, T., A. Cudd, K. Hildenbrand. 1986. Fluorescence studies of the incorporation of *N*-(7-nitrobenz-2-oxa-1,3-diazol-4-yl)-labeled phosphatidylethanolamines into liposomes. *Biochim. Biophys. Acta.* 860:215–228.

Carey, M. C., D. M. Small, and C. M. Bliss. 1983. Lipid digestion and absorption. *Annu. Rev. Physiol.* 45:651–677.

Chattopadhyay, A. 1990. Chemistry and biology of *N*-(-7-nitrobenz-2-oza-1,3-diazol-4-yl)-labeled lipids: fluorescent probes of biological and model membranes. *Chem. Phys. Lipids.* 53:1–15.

Erlinger, S. 1987. Physiology of bile secretion and enterohepatic circulation. *In* Physiology of the Gastrointestinal Tract, 2nd ed. L. R. Johnson, editor. Raven Press, New York. 1557–1580.

Gratton, E., and M. Limkeman. 1983. A continuously variable frequency cross-correlation phase fluorometer with picosecond resolution. *Biophys. J.* 44:315–324.

Hazlett, T. L., K. J. M. Moore, P. N. Lowe, D. M. Jameson, and J. F. Eccleston. 1993. Solution dynamics of $p21^{ras}$ proteins bound with fluorescent nucleotides: a time-resolved fluorescence study. *Biochemistry.* 32:13575–13583.

Hjelm, R. P., Jr., P. Thiyagarajan, and H. Alkan. 1988. A small-angle neutron scattering study of the effects of dilution on particle morphology in mixtures of glycocholate and lecithin. *J. Appl. Cryst.* 21:858–863.

Hjelm, R. P., Jr., P. Thiyagarajan, and H. Alkan. 1990. Small-angle neutron scattering studies of mixed bile salt-lecithin colloids. *Mol. Cryst. Liq. Cryst.* 180A:155–164.

Hoekstra, D. 1982. Fluorescence method for measuring the kinetics of Ca^{2+} induced phase separations in phosphatidylserine-containing lipid vesicles. *Biochemistry.* 21:1055–1061.

Horowitz, A. D., B. Elledge, J. A. Whitsett, and J. E. Baatz. 1992. Effects of lung surfactant proteolipid SP-C on the organization of model membrane lipids: a fluorescence study. *Biochim. Biophys. Acta.* 1107:44–54.

Jameson, D. M., E. Gratton, and R. D. Hall. 1984. The measurement and analysis of heterogeneous emissions by multifrequency phase and modulation fluorometry. *Appl. Spectrosc. Rev.* 20:55–106.

Long, M. A., E. W. Kaler, and S. P. Lee. 1994. Structural characterization of the micelle-vesicle transition in lecithin-bile salt solutions. *Biophys. J.* 67:1733–1742.

Mazer, N. 1990. Quasielastic light scattering studies of aqueous biliary lipid systems and native bile. *Hepatology.* 12:39S-44S.

Milburn, M. P., and K. R. Jeffrey. 1987. Dynamics of the phosphate group in phospholipid bilayers: a P-31 nuclear relaxation time study. *Biophys. J.* 52:791–799.

Milburn, M. P., and K. R. Jeffrey. 1989. Dynamics of the phosphate group in phospholipid bilayers. A. ^{31}P angular dependent nuclear spin relaxation time study. *Biophys. J.* 56:543–549.

Müller, K. 1981. Structural dimorphism of bile salt/lecithin mixed micelles. A possible regulatory mechanism for cholesterol solubility in bile? X-ray structure analysis. *Biochemistry.* 20:404–414.

Müller, K. 1984. Structural aspects of bile salt-lecithin mixed micelles. *Hepatology.* 4:134s–137s.

Nichols, J. W. 1986. Low concentrations of bile salts increase the rate of spontaneous phospholipid transfer between vesicles. *Biochemistry.* 25: 4596–4601.

Nichols, J. W. 1988. Phospholipid transfer between phosphatidylcholine-taurodeoxycholate mixed micelles. *Biochemistry.* 27:3925–3931.

Nichols, J. W., and J. Ozarowski. 1990. Sizing of lecithin-bile salt mixed micelles by size-exclusion high-performance liquid chromatography. *Biochemistry.* 29:4600–4606.

Pascher, I., M. Lundmark, P.-G Nyholm, and S. Sundell. 1992. Crystal structures of membrane lipids. *Biochim. Biophys. Acta.* 1113:339–373.

Schurtenberger, P., and B. Lindman. 1985. Coexistence of simple and mixed bile salt-lecithin micelles: an NMR self-diffusion study. *Biochemistry.* 24:7167–7165.

Schurtenberger, P., N. Mazer, and W. Känzig. 1985. Micelle to vesicle transition in aqueous solutions of bile salt and lecithin. *J. Phys. Chem.* 89:1042–1049.

Shoemaker, D. G., and J. W. Nichols. 1990. Hydrophobic interaction of lysophospholipids and bile salts at submicellar concentrations. *Biochemistry.* 29:5837–5842.

Shoemaker, D. G., and J. W. Nichols. 1992. Interaction of lysophospholipid/taurodeoxycholate submicellar aggregates with phospholipid bilayers. *Biochemistry.* 31:3414–3420.

Small, D. M. 1971. The physical chemistry of cholanic acids. *In* The Bile Acids. P. P. Nair and D. Kritchevsky, editors. Plenum Press, New York. 249–356.

Struck, D. K., D. Hoekstra, and R. E. Pagano. 1981. Use of resonance energy transfer to monitor membrane fusion. *Biochemistry.* 20:4093–4099.

Westergaard, H., and J. M. Dietschy. 1976. The mechanism whereby bile acid micelles increase the rate of fatty acid and cholesterol uptake into the intestinal mucosal cell. *J. Clin. Invest.* 58:97–108.

Wilson, F. A. 1971. Intestinal transport of bile acids. *Am. J. Physiol.* 241:G83–G92.

Wilson, F. A. 1991. Intestinal transport of bile acids. *In* Handbook of Physiology—The Gastrointestinal System IV. S. G. Schultz, J. G. Forte, and B. B. Rauner, editors. Waverly, New York. 389–404.